Statistical thermodynamics of bond torsional modes: Tests of separable, almost-separable, and improved Pitzer–Gwinn approximations

Benjamin A. Ellingson and Vanessa Audette Lynch
Department of Chemistry, University of Minnesota, Minneapolis, Minnesota 55455-0431
and Supercomputing Institute, University of Minnesota, Minneapolis, Minnesota 55455-0431

Steven L. Mielke[a)]
Department of Chemistry, Northwestern University, Evanston, Illinois 60208-3113

Donald G. Truhlar[b)]
Department of Chemistry, University of Minnesota, Minneapolis, Minnesota 55455-0431
and Supercomputing Institute, University of Minnesota, Minneapolis, Minnesota 55455-0431

Practical approximation schemes for calculating partition functions of torsional modes are tested against accurate quantum mechanical results for H_2O_2 and six isotopically substituted hydrogen peroxides. The schemes are classified on the basis of the type and amount of information that is required. First, approximate one-dimensional hindered-rotator partition functions are benchmarked against exact one-dimensional torsion results obtained by eigenvalue summation. The approximate one-dimensional methods tested in this stage include schemes that only require the equilibrium geometries and frequencies, schemes that also require the barrier heights of internal rotation, and schemes that require the whole one-dimensional torsional potential. Then, three classes of approximate full-dimensional vibrational-rotational partition functions are calculated and are compared with the accurate full-dimensional path integral partition functions. These three classes are (1) separable approximations combining harmonic oscillator-rigid rotator models with the one-dimensional torsion schemes, (2) almost-separable approximations in which the nonseparable zero-point energy is used to correct the separable approximations, and (3) improved nonseparable Pitzer–Gwinn-type methods in which approaches of type 1 are used as reference methods in the Pitzer–Gwinn approach. The effectiveness of these methods for the calculation of isotope effects is also studied. Based on the results of these studies, the best schemes of each type are recommended for further use on systems where a corresponding amount of information is available. © *2006 American Institute of Physics*. [DOI: 10.1063/1.2219441]

I. INTRODUCTION

Internal rotation, also called hindered rotation or torsion, where one part of a molecule rotates with respect to another, is a type of vibrational mode for which the harmonic approximation may be seriously in error.[1] Furthermore, the usual treatment of anharmonicity in terms of cubic and quartic force constants[2,3] may fail to capture the essential characteristics of the anharmonic corrections. Approximations in terms of a separable one-dimensional Hamiltonian with periodic boundary conditions have been available for a long time[4,5] but remain a subject of continued study.[6–29] The quantitative validity of such treatments is, however, unknown because internal rotations of real molecules are coupled to other vibrations and overall rotation, so if one compares calculated energy levels or calculated thermodynamic functions with experiment, one cannot unambiguously ascribe any deviations to specific modes, and the interpretation is also complicated by possible inaccuracies in the potential energy function and possibly even in the experiment.

One way to eliminate the latter two complications is to calculate converged quantum mechanical (QM) thermodynamic functions for a known, realistic potential energy surface of a small molecule, and then to use these to test the kinds of approximations that one can use for practical applications on large molecules and transition states, where accurate QM calculations cannot be carried out. However, even for small molecules, the calculation of converged thermodynamic functions, which requires, in practice, the calculation of converged QM partition coefficients (or, equivalently, absolute free energies), is difficult, especially for molecules with large-amplitude vibration, such as internal rotations. Recently, however, for the first time, converged QM partition functions and free energies have been calculated for a molecule with a torsion,[30] in particular, for the H_2O_2 molecule, which is the simplest molecule with a torsion. In a subsequent article,[31] we extended these calculations to D_2O_2, HOOD, $H_2{}^{18}O_2$, $H^{18}OOH$, $D^{18}OOH$, and $H^{18}OOD$, where H denotes ^1H and O denotes ^{16}O. In the present article, we test several approximation schemes, including separable treatments of vibrations and rotations against converged nonseparable partition functions for molecules with torsions, in particular, for the seven molecules just mentioned. To aid in the

[a)]Electronic mail: slmielke@sbcglobal.net
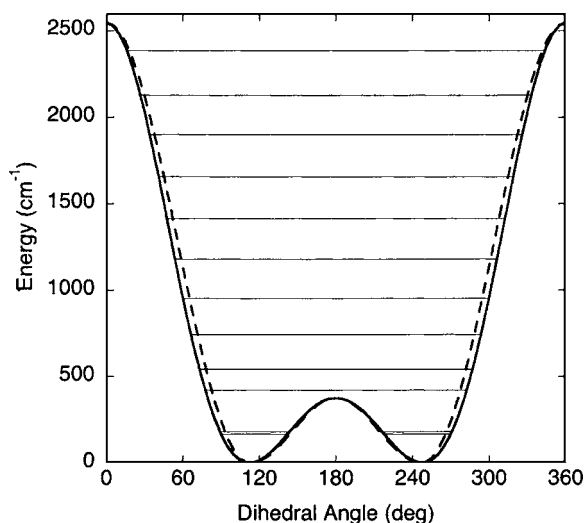[b)]Electronic mail: truhlar@chem.umn.edu

FIG. 1. The potential energy along the effective torsional coordinate for H_2O_2 as given by Eq. (1) (solid curve) and the segmented reference potential (dashed curve) are plotted as a function of ϕ. The H_2O_2 eigenvalue spectrum of the potential of Eq. (1) is also displayed.

analysis, we also present some tests of one-dimensional torsion treatments against accurate one-dimensional results, and we also consider almost-separable approximations in which only the zero-point energy includes nonseparable effects. Finally, we consider the improvements that such separable approximations and almost-separable approximations can provide when these are used as reference models in place of the usual harmonic approximation for the quantum correction factor of the Pitzer–Gwinn approximation.

II. SYSTEM AND POTENTIAL EXPRESSIONS

All multidimensional calculations in this paper, and in our prior path integral calculations,[30,31] are based on the potential energy surface of Koput *et al.*[32] All calculations involving the one-dimensional torsional potential use the fit of Koput *et al.*[32] along the minimum-energy torsion path (i.e., where the energy is minimized with respect to all coordinates other than the torsion angle ϕ). This fit is given by

$$V/\text{cm}^{-1} = 811.305\,354\,6 + 1037.4\cos(\phi)$$
$$+ 647.2\cos(2\phi) + 46.9\cos(3\phi) + 2.7\cos(4\phi),$$
$$(1)$$

where ϕ is the torsion angle. A plot of this curve is shown in Fig. 1. Atomic mass values for H, D, ^{16}O, and ^{18}O are taken to be 1.007 825 03, 2.014 101 78, 15.994 914 6, and 17.999 160 amu, respectively. The equilibrium configuration for the full-dimensional (full-D) potential occurs with $R_{OH} = 0.962\,65$ Å, $R_{OO} = 1.452\,48$ Å, HOO angles of 99.9086°, and a dihedral angle of $\phi = 112.456°$, and the one-dimensional (1D) potential of Eq. (1) has an equilibrium configuration with $\phi = 112.504°$.

Some methods approximate the one-dimensional hindered-rotator problem with a simple model potential of the form

$$V = \frac{W}{2}(1 - \cos M\phi),\qquad(2)$$

where W is the height of the potential barrier, M is the number of minima in the range $[0, 2\pi]$, and ϕ is a coordinate that parametrizes the rotational motion. For a potential of the form of Eq. (2) with a geometry-independent moment of inertia, the barrier height W, moment of inertia I, and one-dimensional torsional frequency $\bar{\omega}$ are interrelated by

$$\bar{\omega} = M\left(\frac{W}{2I}\right)^{1/2},\qquad(3)$$

but for more general potentials Eq. (3) need not be an accurate approximation. For hydrogen peroxide and its isotopologs, $M = 2$, and various methods use differing values for $\bar{\omega}$, W, and I as discussed below.

III. THEORY

The theoretical methods used to obtain the accurate partition functions used to benchmark the approximation methods in this paper have been presented previously[30,31] and they will not be repeated here.

We will consider a large number of methods in this paper; in order to aid the reader in distinguishing these methods we provide a glossary of acronyms in Table I.

Many of the approximate methods considered in the present paper (all methods introduced prior to Sec. V.B) assume separable rotation, that is, the partition function is approximated by

$$Q = Q_{\text{vib}}(T)Q_{\text{rot}}(T),\qquad(4)$$

where the factors are, respectively, the vibrational and rotational partition functions and T denotes temperature. In general, the partition function depends on the zero of energy, and this is often[1,33] taken as the ground-state energy. However, in order to evaluate thermodynamic functions such as standard-state enthalpies and standard-state free energies from potential energy surfaces (PESs), we need to calculate the partition function with the zero of energy equal to the potential energy at the equilibrium structure of the molecule, and this is the zero of energy we use in the present paper (except, as noted below, when we use the other zero of energy[1,33] for an intermediate result to simplify the presentation—in such a case the quantity with the zero of energy at the ground state will always have a tilde).

In previous papers,[30,31] we compared five methods for calculating the rotational partition functions of H_2O_2 and six of its isotopologs, and we found that they all agree with one another within 2% for all molecules studied here over the entire 300–2400 K temperature range. Therefore, when calculating the $Q_{\text{rot}}(T)$, we will simply use one of these methods, namely, the quantum mechanical symmetric-top approximation with moments of inertia evaluated from the equilibrium structure (called $Q_{\text{rot}}^{\text{sym},e}$ in previous work[30,31] but simply called Q_{rot} in the present article).

In the following sections we consider approximations for Q_{vib}. We will divide these into separable approximations, considered in Sec. IV, and nonseparable approximations,

TABLE I. Glossy of acronyms.

AS	The method of Ayala and Schlegel (Ref. [14]); see Sec. IV.C.2.
C scheme	Curvilinear moment of inertia scheme of Pitzer (Ref. [5]).
CAF scheme	Curvilinear-averaged-frozen scheme for effective moment of inertia; see Sec. IV.E.
CAR scheme	Curvilinear-averaged-relaxed scheme for effective moment of inertia; see Sec. IV.E.
CT	Chuang-Truhlar (Ref. [18]) interpolatory methods for obtaining the parameters of a reference model; see Sec. IV.B.
CW	CT method that uses the C scheme I and the barrier height to calculate the required frequency.
$C\omega$	CT method that uses the C scheme I and the harmonic frequency.
FR	Free rotor; see Eqs. [(19)] and [(23)].
HO	Harmonic oscillator.
HO+T	HO for nontorsion modes and a separable anharmonic treatment of the torsion.
I	The effective reduced moment of inertia associated with the torsional motion.[a]
IW	CT method that uses the effective reduced moment of inertia and the barrier height to calculate the required frequency, more typically referred to as CW or RW in order to specify whether the R scheme or C scheme I has been used.
$I\omega$	CT method that uses the effective reduced moment of inertia and the harmonic frequency, more typically referred to as $C\omega$ or $R\omega$ to specify whether the R scheme or C scheme I has been used.
IRPG	Improved-reference Pitzer–Gwinn approximation; see Sec. V.B.
MC-HO	Multiconformer harmonic oscillator approximation; see Eq. [(9)].
MPG	Modified Pitzer–Gwinn method (used here only for the torsional coordinate); see Eq. [(41)].
PG	The Pitzer–Gwinn approximation. This notation is reserved for calculations where the classical approximation involves all the coupling of the full-D potential.
RPG	Torsional Pitzer–Gwinn approximation using a single cosine reference potential. In the present article the reference potential is obtained by requiring the barrier height to be equal to the mean value of the barrier heights of the accurate 1D potential.
R scheme	A "rectilinear" moment of inertia scheme (Ref. [9]).
RW	CT method that uses the R scheme I and the barrier height to calculate the required frequency.
$R\omega$	Method for obtaining reference model parameters by using the R scheme I and the harmonic frequency.
SAS	Segmented Ayala–Schlegel method; see Sec. IV.C.3.
SRC	Segmented reference classical method; see Sec. IV.C.3.
SRPG	Segment reference Pitzer–Gwinn approximation; see Sec. IV.C.3.
SR-TDPPI-HS	The TDPPI-HS method applied to a segmented reference potential.
TDPPI-AS	Torsional displaced-points path integral method with anharmonic sampling.
TDPPI-HS	Torsional displaced-points path integral method with harmonic sampling.
TES	Torsional eigenvalue summation; see Sec. IV.D.1.
TPG	Torsional Pitzer–Gwinn approximation, i.e., the PG approximation used only for the 1D torsional potential.
WK	The Wigner–Kirkwood approximation; see Eq. [(40)].
Z	When appended to any other method acronym this indicates that an accurate ZPE is used.
ZPE	Zero-point energy.

[a]I is a mathematical symbol, not an acronym, but it is included here to avoid confusion.

considered in Sec. V. The main reason that we consider a variety of methods is that they require different amounts and kinds of data, and some of the data are not as readily available as other kinds of data. For example, the accurate one-dimensional potential may be unavailable or too expensive to calculate if the potential is determined by high-level direct electronic structure calculations. Or it may be inefficient to calculate this along a reaction coordinate if one is calculating a free energy profile as a function of a reaction coordinate. We therefore categorize the methods in terms of a hierarchy of data requirements.

Methods that require geometries and frequencies. The

minimum amount of data necessary for thermochemical calculations on molecules is the geometry and the frequencies of all the local minima. For H_2O_2 and its isotopic analogs, since the two local minima on the potential function correspond to mirror-image geometries, only one set of frequencies needs to be considered.

Methods that require geometries, frequencies, and barrier heights. At a next higher level, one also knows the barrier heights between the local minima. These barrier heights, like the geometries of the minima, are independent of isotopic substitution. There are two nonequal barrier heights for H_2O_2 as shown in Fig. 1.

Methods that require the whole 1D potential. Some methods require not just the energies of the local minima and maxima along the torsion but the full one-dimensional torsion potential as a function of the geometry.

Methods that require the zero-point energy (ZPE). These methods are calculated by replacing the ZPE used in any method by a more accurate ZPE. Methods employing this strategy are called *Z*-type methods. The calculation of the ZPE for the separable 1D potential is explained in Sec. IV.F. The calculation of the ZPE for the full-dimensional problem is an anharmonic coupled-vibrational-mode calculation, which is usually too computationally demanding to be available. Although the accurate coupled-mode ZPE is not usually available, consideration of *Z*-type methods provides insight into the sources of error in the separable calculations, and it is worthwhile to consider this kind of method for that reason, if for no other. However, special techniques are available for computing ground vibrational states because they are nodeless,[34–36] and it is interesting to ask how much it would improve the quality of the result to also calculate an accurate ground-state vibrational energy.

Methods that require the multidimensional potential. Improved-reference Pitzer–Gwinn methods, which are defined in Sec. V.B, require the knowledge of the entire full-dimensional nonseparable potential energy surface (V_{full}) or at least those parts of it that make non-negligible contributions to the classical partition function.

Methods that require the multidimensional ZPE or the multidimensional potential are nonseparable. The former still involve separable rotation, but do not assume separable vibrational modes. The method involving V_{full} does not even assume separable rotation.

IV. SEPARABLE APPROXIMATIONS

The simplest expression for the vibrational partition function is obtained by making the harmonic oscillator (HO) approximation for all modes. Another very general approach is to make the harmonic oscillator approximation for all nontorsional modes but to treat the torsion anharmonically; this will be called a harmonic oscillator plus torsion (HO+T) approximation. All separable approximations considered in the present paper are of the HO+T variety. The QM harmonic oscillator approximation to the vibrational partition function is

$$Q_{vib}^{HO} = \prod_{m=1}^{F} Q_m^{HO}, \tag{5}$$

where m labels the vibrational mode and F is the number of vibrational modes, which is 6 for the molecules considered here. The individual HO partition function for each mode m is given by

$$Q_m^{HO} = \frac{e^{-\beta\hbar\omega_m/2}}{1 - e^{-\beta\hbar\omega_m}}, \tag{6}$$

where β is $(kT)^{-1}$, k is Boltzmann's constant, and ω_m is the harmonic vibrational frequency of mode m.

For H_2O_2, mode 4 is a torsion. For convenience we retain the H_2O_2 numbering of the modes for isotopically substituted cases, so the torsion is labeled mode 4 in all cases. In the rest of this section we consider HO+T approximations where mode 4 is specially treated as a torsion. Then Eq. (5) is replaced by

$$Q_{vib}^{HO+T} = Q_{sb}^{HO} Q_{tor}, \tag{7}$$

where Q_{tor} is a hindered-rotator partition function and Q_{sb}^{HO} is the HO stretch-bend partition function given by

$$Q_{sb}^{HO} = \prod_{m=1-3,5,6} Q_m^{HO}. \tag{8}$$

In the rest of this section, ω_4 is denoted as ω. We note that $\omega/2\pi c$ ranges from 381.9 cm^{-1} for H_2O_2 to 279.4 cm^{-1} for D_2O_2.

Special care must be taken when treating torsions with distinguishable minima. Hindered-rotator methods are typically defined for indistinguishable minima, such as those in ethane or CH_2D-CH_3. However, molecules such as CH_2D-CH_2D, H_2O_2, and HOOD have distinguishable minima. When all distinguishable minima are accounted for at the harmonic level of approximation[18,31] we will refer to this as a multiconformer HO (MC-HO) treatment. In this method, the harmonic oscillator approximation for a torsional mode with $m=t$ is given by

$$Q_{tor}^{MC-HO} = \sum_{j=1}^{P} \frac{e^{-\beta(U_j + \hbar\omega_{tj}/2)}}{1 - e^{-\beta\hbar\omega_{tj}}}, \tag{9}$$

where P is the number of distinguishable minima, ω_{tj} is the harmonic frequency at minimum j of torsional mode t (in our case, $t=4$), and U_j is the energy of well j of this mode relative to the lowest well of this mode.

We note that molecules that have indistinguishable minima require a symmetry number σ so that indistinguishable configurations are not overcounted. (Note that this is the symmetry number for internal rotation and should not be confused with the symmetry number in Q_{rot}.) In this paper we also employ the convention of including the symmetry number in classical formulas so that quantum mechanically indistinguishable regions of phase space are not overcounted. For example, ethane requires $\sigma=3$ because of the three indistinguishable minima. (Thus when we refer to the partition function for H_2O_2 or any of its isotopologs, we mean the integral over all phase space divided by σ.) For H_2O_2 and its various isotopologs, the two minima are nonsuperimposable

mirror images, which requires $\sigma=1$. Therefore, $P=2$, $U_1=U_2=0$, and $\omega_{t1}=\omega_{t2}=\omega$. The net result in these systems is that the simple harmonic oscillator partition function will be doubled: $Q_{\text{tor}}^{\text{MC-HO}}$ equals $2Q_4^{\text{HO}}$. Similar symmetry considerations apply to the other isotopologs so that all molecules considered in this paper have distinguishable minima with σ equal to unity, $P=2$, $U_1=U_2=0$, and $\omega_{t1}=\omega_{t2}$.

IV.A. Approximations derived from the torsional Pitzer–Gwinn-type methods

In their seminal paper, Pitzer and Gwinn[4] provided accurate numerical solutions of the one-dimensional hindered-rotator problem for a simple model potential of the form in Eq. (2). The Schrödinger equation for this problem is

$$-\frac{\hbar^2}{2I_{\text{tor}}}\frac{d^2\Psi}{d\phi^2} + V\Psi = E\Psi, \tag{10}$$

where E is the energy and I_{tor} is the reduced moment of inertia. We will make use of "reference models" in which Eq. (10) is used with I_{tor} assumed to be independent of ϕ or with I_{tor} replaced by an effective or average value I. For such a reference model, Eq. (10) may be transformed into Hill's equation and solved for a set of eigenvalues.[4] Partition functions may then be obtained by direct eigenvalue summation, and free energies and entropies may be obtained from these. Pitzer and Gwinn[4] tabulated such thermodynamic functions for a wide range of parameters.

They also presented[4] a simple scheme, now known as the Pitzer–Gwinn (PG) approximation, for estimating the accurate quantum mechanical partition function by adjusting a classical partition function $Q^{\text{classical}}$ with a quantum correction obtained at the harmonic level. This approximation is especially useful for approximating mode-coupling effects,[37] and for consistency with previous work, we reserve the simple name PG approximation for such applications where the classical partition function is multidimensional. In this section, we consider one-dimensional applications of their method to the torsion. This is called the torsional Pitzer–Gwinn (TPG) approximation, i.e.,

$$Q_{\text{tor}}^{\text{TPG}} = \exp(-\beta\hbar\bar{\omega}/2)\left(\frac{\widetilde{Q}_{\text{tor}}^{\text{HO}}(\bar{\omega})}{Q_{\text{tor}}^{\text{CHO}}(\bar{\omega})}\right)Q_{\text{tor}}^{\text{classical}}, \tag{11}$$

where $\bar{\omega}$ indicates the frequency associated with the minimum of the 1D torsional potential, that is,

$$\bar{\omega} = (k/I)^{1/2}, \tag{12}$$

where

$$k \equiv \left.\frac{d^2V}{d\phi^2}\right|_{\phi=\phi_c} \tag{13}$$

and where ϕ_e is the equilibrium value of the torsion angle. [Note carefully the distinction between $\bar{\omega}$ and the normal mode torsional frequencies ω_{ti} associated with the torsional motion of a full-D potential that $V(\phi)$ may be intended to model.] $Q_{\text{tor}}^{\text{CHO}}$ (which equals $1/\hbar\beta\bar{\omega}$) and $\widetilde{Q}_{\text{tor}}^{\text{HO}}$ are, respectively, the classical and QM harmonic oscillator partition functions for the torsion (a tilde indicates a partition function

that is relative to the ground-state energy), and $Q_{\text{tor}}^{\text{classical}}$ is the accurate classical partition function for the torsion,

$$Q_{\text{tor}}^{\text{classical}} = \sqrt{\frac{IkT}{2\pi\hbar^2}}\int_0^{2\pi/\sigma}d\phi\,\exp(-\beta V[\phi]). \tag{14}$$

We will restrict use of the TPG notation to cases where the accurate classical partition function of the true potential is calculated. We note that the original PG approximation was presented in a notation with the zero of energy at the ground-state energy, and that Eq. (11) has been adjusted to the current convention in which Q^{TPG} is relative to a zero of energy at the classical minimum.

The original torsional Pitzer–Gwinn approximation of Eq. (11) is appropriate when the quantum effects for all wells can be reasonably approximated by a single frequency, as is the case for the present set of applications. If individual wells have distinct frequencies, one would use

$$Q_{\text{tor}}^{\text{TPG}} = \sum_{j=1}^{P}\exp(-\beta\hbar\bar{\omega}_j/2)\frac{\widetilde{Q}_{\text{tor}}^{\text{HO}}(\bar{\omega}_j)}{Q_{\text{tor}}^{\text{CHO}}(\bar{\omega}_j)}\sqrt{\frac{IkT}{2\pi\hbar^2}}$$
$$\int_{\Omega_j}d\phi\,\exp(-\beta V[\phi]), \tag{15}$$

where Ω_j is the domain of well j.

The TPG and classical approximations are two examples of HO+T approximations. The following subsections (Secs. IV.B–IV.F) are entirely devoted to other separable treatments of Q_{tor} that may be used in the HO+T treatment.

IV.B. Methods that require geometries and frequencies

These types of methods include the MC-HO method defined above and the CT-Cω method defined below. The MC-HO method can be considered to be the simplest example of a HO+T method since it takes account of distinguishable minima along the torsion. It provides an appropriate partition function when both kT/W and $\hbar\omega/W$ are small. Another method that only requires the geometries and frequencies is the CT-Cω method described next.

Truhlar[9] and Chuang and Truhlar[18] (CT) recommended a number of approximate schemes in which the partition function for torsion is estimated via

$$Q_{\text{tor}} = Q_{\text{tor}}^{\text{MC-HO}}\tanh\left(\frac{Q_{\text{FR}}}{Q^{\text{I}}}\right), \tag{16}$$

where $Q_{\text{tor}}^{\text{MC-HO}}$ is given by Eq. (9) and Q^{I} (the "intermediate" approximation defined below) and Q_{FR} (the free-rotator approximation) are intended to model the partition function for intermediate-T values and for the high-T, free-rotator limit, respectively.

In general, the moment of inertia varies with the torsion coordinate; in such cases Q_{FR} is given by

$$Q_{\text{FR}} \approx Q_{\text{FR}}^{\text{classical}} = \left(\frac{kT}{2\pi\hbar^2}\right)^{1/2}\int_0^{2\pi/\sigma}[I_{\text{tor}}(\phi)]^{1/2}d\phi. \tag{17}$$

Chuang and Truhlar[18] suggested that if there are P distinguishable minima in $V(\phi)$, one might estimate an effective reduced moment of inertia as the mean of the moments of

inertia $I_{\text{tor},i}$ at each of the P distinct minima i, i.e.,

$$I \approx \frac{1}{P} \sum_{i=1}^{P} I_{\text{tor},i}, \tag{18}$$

and use this moment of inertia in

$$Q_{\text{FR}}^{\text{classical}} = \frac{(2\pi I k T)^{1/2}}{\hbar \sigma}. \tag{19}$$

A number of different estimation procedures are available to obtain the $I_{\text{tor},i}$ values; these will be considered in more detail in Sec. IV.E.

In the intermediate-temperature regime, where kT is higher than $\hbar\omega$ but less than the barrier height W, the partition function is reasonably approximated by

$$Q^{\text{I}} = \sum_{j=1}^{P} \frac{e^{-\beta U_j}}{\hbar \beta \omega_{tj}}, \tag{20}$$

which is the high-temperature limit of Eq. (9).

As written, Eq. (16) depends explicitly on the ω_{tj} and I values but has only an implicit dependence on the barrier heights W. Recall that for our problem both ω_{tj} (that is, ω_{41} and ω_{42}) are the same and are called ω. When Eq. (16) is approximated directly in terms of I and ω we will denote this as the Cω scheme.

If I were independent of ϕ, the Cω scheme would be asymptotically correct in the high-T limit, which depends only on I and T, and it has reasonable behavior in the low-T limit, which depends on the harmonic frequencies ω_{tj}; but for general potentials the Cω scheme is not expected to necessarily perform well in the intermediate-T regime where Q_{tor} is sensitive to the barrier heights. In Sec. IV.C, we consider methods that are intended to improve on this aspect.

IV.C. Methods that require geometries, frequencies, and barrier heights

This section contains the CT-CW, CT-ωW, RPG, SRC, SRPG, and SAS methods. A seventh scheme, the SR-TDPPI-HS method, appears in Sec. IV.D.3 even though it only needs the geometries, frequencies, and barrier heights. This section starts with the continuation of the Chuang and Truhlar[18] methods as they are extended to also use barrier heights.

IV.C.1. Interpolatory treatments

In an attempt to obtain approximations that might be more accurate at intermediate temperatures, Chuang and Truhlar[18] considered two other approaches, the CW and ωW methods, where best estimates of either I (in the ωW method) or the ω_{tj} (in the CW method) are replaced by effective values calculated from barrier heights via Eq. (3). One complication with these approaches is that the left and right barriers for a particular well are typically not equal; in such cases Chuang and Truhlar[18] suggested that the median of the left and right barriers be used as the effective value of W associated with a particular well, i.e.,

$$W_j^{\text{eff}} = (W_j^L + W_j^R)/2, \tag{21}$$

and we will follow this suggestion.

In the EPAPS supplement, the Rω and RW methods of CT are also considered; these methods use a different (and apparently less generally reliable) value for I; see Sec. IV.E for more information on the R method for calculating the moment of inertia.

IV.C.2. The RPG approximation and extensions

For the special case of a potential of the form of Eq. (2), the classical hindered-rotator partition function of Eq. (14) may be analytically integrated to yield

$$Q_{\text{tor}}^{\text{classical}} = Q_{\text{FR}}^{\text{classical}} \exp(-\beta W/2) I_0(\beta W/2), \tag{22}$$

where $Q_{\text{FR}}^{\text{classical}}$ is the classical free-rotator partition function in Eq. (19) and $I_0(\beta W/2)$ is a modified Bessel function. Note that the quantum mechanical free-rotator partition function,

$$Q_{\text{FR}}^{\text{QM}} = \sum_{n=-\infty}^{\infty} \exp\left(\frac{-n^2 \hbar^2 \beta}{2I} \right), \tag{23}$$

is virtually identical to that of Eq. (19) except at very low temperatures, so Eq. (19) is usually just referred to as the free-rotator partition function or Q_{FR} rather than as the classical approximation for a free rotator.

Potentials for realistic systems will differ from the form of Eq. (2); however, in many situations Eq. (2) is a reasonable approximation. When the true potential is approximated by a fit to the form of Eq. (2) and then Eqs. (11) and (22) are used, we will refer to this as a reference PG (RPG) approximation to distinguish it from the true TPG approximation. Combining Eqs. (11) and (22) yields a convenient expression for the RPG partition function for a torsion,

$$Q_{\text{tor}}^{\text{RPG}} = \exp(-\beta\hbar\bar{\omega}/2) \left[\frac{\tilde{Q}_{\text{tor}}^{\text{HO}}(\bar{\omega})}{Q_{\text{tor}}^{\text{CHO}}(\bar{\omega})} \right] Q_{\text{FR}}$$
$$\times \exp(-\beta W/2) I_0(\beta W/2). \tag{24}$$

A number of different strategies are possible for fitting the true potential to the form of Eq. (2); in our numerical tests of the RPG method in the present article we will only consider the use of a value of W that is the average of the two barrier heights observed for the potential of Eq. (1).

When modeling the contribution of a torsion to a full-D partition function using either the TPG or RPG expressions, the quantum effects may be better characterized by the torsional frequencies of the full-D problem, ω_{tj}, rather than the $\bar{\omega}_j$. We will adopt this further modification of the TPG and RPG forms in all of our tests.

McClurg *et al.*[12] (MFG) considered a correction to the RPG form to account for anharmonicity in the ZPE. They suggested that for barriers W that are large compared with $\hbar\bar{\omega}$, the zero-point energy might be expressed using

$$E_0 = \hbar\bar{\omega}/2 - \frac{\hbar\bar{\omega}}{16r} + O(r^{-2}), \tag{25}$$

where

$$r = \frac{W}{\hbar\bar{\omega}}, \tag{26}$$

and recommended a Padé approximant,

$$\Delta E^{\mathrm{MFG}} = -\frac{\hbar\bar{\omega}}{2 + 16r}, \tag{27}$$

to estimate the ZPE anharmonicity for both large and small barrier heights. Their adjusted partition function function can be written as

$$Q^{\mathrm{MFG}} = \exp(-\beta\Delta E^{\mathrm{MFG}})Q^{\mathrm{RPG}}. \tag{28}$$

McClurg et al.[12] warned that their method may not be appropriate for molecules such as H_2O_2 that possess asymmetrical wells due to widely differing barrier heights. We note that McClurg et al.[12] prefer to use the expression relating $\bar{\omega}$, W, and I in Eq. (3) to eliminate the explicit dependence on I in their final result,

$$Q^{\mathrm{MFG}}_{\mathrm{tor}} = \exp(-\beta\Delta E^{\mathrm{MFG}})(\pi\beta W)^{1/2}Q^{\mathrm{HO}}_{\mathrm{tor}}(\bar{\omega})$$
$$\times \exp\left(\frac{-\beta W}{2}\right)I_0\left(\frac{\beta W}{2}\right). \tag{29}$$

McClurg et al. further substituted ω_{tj} for $\bar{\omega}$ in Eq. (29), but in light of Eq. (28), this corresponds to changing the effective moment of inertia, which changes the high-temperature limit so it no longer agrees with the RPG high-temperature limit.

Ayala and Schlegel[14] (AS) attempted to find a correction factor to adjust the RPG scheme to better match the accurate partition functions tabulated by Pitzer and Gwinn.[4] Their recommended expression is of the form

$$Q^{\mathrm{AS}} = \frac{1 + P_2 \exp[-\beta W/2]}{1 + P_1 \exp[-\beta W/2]}Q^{\mathrm{RPG}}, \tag{30}$$

where P_1 and P_2 are fifth order polynomial functions of $x \equiv 1/Q_{\mathrm{FR}}$ and $y \equiv \beta W/2$ given by[14,38,39]

$$P_1 = 0.003\,235x - 0.026\,252x^2 + 0.110\,460x^3 - 0.203\,340x^4 + 0.130\,633x^5 - 0.010\,112y^{0.5} + 0.650\,122xy^{0.5}$$
$$+ 0.067\,112x^2y^{0.5} + 0.088\,807x^3y^{0.5} - 0.014\,290x^4y^{0.5} - 0.364\,852y + 0.913\,073xy - 0.021\,116x^2y - 0.092\,086x^3y$$
$$- 0.415\,689y^{1.5} - 1.128\,961xy^{1.5} + 0.233\,009x^2y^{1.5} + 0.421\,344y^2 + 0.505\,139xy^2 - 0.215\,088y^{2.5} \tag{31}$$

and

$$P_2 = -0.067\,113x + 0.772\,485x^2 - 3.067\,413\,1x^3 + 4.595\,051x^4 - 2.101\,341x^5 + 0.015\,800y^{0.5} + 0.102\,119xy^{0.5}$$
$$- 0.555\,270x^2y^{0.5} - 1.125\,261x^3y^{0.5} + 0.071\,884x^4y^{0.5} - 0.397\,330y + 2.284\,956xy + 0.850\,046x^2y - 0.174\,240x^3y$$
$$- 0.451\,875y^{1.5} - 2.136\,226xy^{1.5} + 0.303\,469x^2y^{1.5} + 0.470\,837y^2 + 0.675\,898xy^2 - 0.226\,287y^{2.5}. \tag{32}$$

IV.C.3. Segmented methods

If the hindered-rotator potential does not closely resemble the form of Eq. (2), it may be convenient to decompose the partition function into a sum of contributions from particular wells and to fit the potential between each peak and minimum using a simple cosine line shape. This segmented reference potential is compared with the accurate 1D potential in Fig. 1. For each well, the contribution may be divided into the part to the left of the minimum and the part to the right of the minimum, and each part of the classical partition function may be evaluated analytically. We will refer to this as the segmented reference classical (SRC) approximation, and it yields

$$Q^{\mathrm{SRC}} = \sum_j Q^{\mathrm{SRC}}_j, \tag{33}$$

where

$$Q^{\mathrm{SRC}}_j = \exp(-\beta U_j)Q_{\mathrm{FR},j}$$
$$\times \left[\frac{(\phi_j - \phi_j^L)}{2\pi}\exp(-\beta W_j^L/2)I_0(\beta W_j^L/2) \right.$$
$$\left. + \frac{(\phi_j^R - \phi_j)}{2\pi}\exp(-\beta W_j^R/2)I_0(\beta W_j^R/2) \right], \tag{34}$$

where the sum is over the number of wells, U_j is the energy of the local minimum (of V) centered at ϕ_j relative to the energy at the global minimum, W_j^L and W_j^R are the left and right barrier heights located at ϕ_j^L and ϕ_j^R, respectively, and

$$Q_{\mathrm{FR},j} = \frac{\sqrt{2\pi I_j kT}}{\hbar\sigma}. \tag{35}$$

Quantum effects may be approximated by the Pitzer–Gwinn approximation to yield the segmented reference Pitzer–Gwinn (SRPG) method. The general solution is

$$Q^{\mathrm{SRPG}}_{\mathrm{tor}} = \sum_j \frac{Q_j^{\mathrm{HO}}(\omega_j)}{Q_j^{\mathrm{CHO}}(\omega_j)}Q_j^{\mathrm{SRC}}. \tag{36}$$

A simple version of the SRPG scheme has been used in the past by Katzer and Sax.[23]

The Ayala–Schlegel method[14] has an analogous segmented approach, which we will refer to as the segmented Ayala–Schlegel (SAS) method, in which each occurrence of $\exp(-\beta W_j/2)$ in Eq. (34) is replaced by a term like

$$\exp(-\beta W_j/2)\frac{1 + P_2(I_j, W_j)\exp(-\beta W_j/2)}{1 + P_1(I_j, W_j)\exp(-\beta W_j/2)},$$

where P_1 and P_2 are given by Eqs. (31) and (32). The AS scheme is typically more accurate than the RPG scheme, but it is not clear that the SAS scheme is systematically more accurate than the SRPG scheme because the polynomials have not been parameterized for general potentials.

IV.D. Methods that require the accurate 1D potential

Two methods, TPG and classical, that require the whole 1D potential were already explained in the first part of Sec. IV. This section explains five more methods that use the whole potential, namely, the TES, WK, MPG, TDPPI-HS, and TDPPI-AS methods.

IV.D.1. Torsional eigenvalue summation

For one-dimensional torsional potentials that deviate significantly from the simple form of Eq. (2), a convenient strategy is to try to represent the potential with a higher-order Fourier series,

$$V = b_0 + \sum_{j=1}^{j_{max}} b_j \cos(n\phi). \tag{37}$$

The importance of additional Fourier terms in the torsional potential beyond the one included in Eq. (2) has long been recognized.[40–45] If we assume that $I_{tor}(\phi)$ is independent of the torsion coordinate, which (as discussed further below) holds very well for the case of H_2O_2 (but does not always hold well), then the eigenfunctions of the Hamiltonian may be readily represented in a basis of the form $(1/\sqrt{2\pi})\exp(ik\phi)$ and diagonalized to yield the full spectrum. Partition functions may then be computed by eigenvalue summation. Matrix elements of the Hamiltonian in this basis may be analytically integrated using

$$\int_0^{2\pi} d\phi e^{ik\phi} \cos(n\phi) = 2\pi \quad \text{if } k = n = 0$$

$$= \pi \quad \text{if } k = n \neq 0$$

$$= 0 \quad \text{if } k \neq n \tag{38}$$

to obtain

$$H_{jk} = k^2\hbar^2/2I + b_0, \quad \text{if } j = k$$

$$= b_{|j-k|}/2, \quad \text{if } j \neq k. \tag{39}$$

This yields a symmetric real banded matrix (with bandwidth equal to $2j_{max}+1$); thus, for reasonable expansion lengths, diagonalization is often an affordable option. We will denote calculations using eigenvalue summation for the torsional coordinate as TES (for torsional eigenvalue summation).

IV.D.2. Approximations based on the Wigner–Kirkwood expression

For one-dimensional problems accurate quantum path integral methods are much more expensive than direct diagonalization, but it may be economical to carry out

numerical integration of the classical approximation, i.e., Eq. (14), or of the semiclassical Wigner–Kirkwood (WK) approximation,[46,47]

$$Q_{tor}^{WK} = \frac{(I/2\pi\beta)^{1/2}}{\hbar} \int_0^{2\pi/\sigma} d\phi \exp(-\beta V[\phi])$$

$$\times \left[1 + \frac{\hbar^2\beta^2}{12I}\left(-\frac{d^2V(\phi)}{d\phi^2} + \frac{\beta}{2}\frac{dV(\phi)}{d\phi}\right)\right], \tag{40}$$

where we have retained terms only through second order in the WK expansion. Hui-yun[7] has suggested a modified PG (MPG) approximation in which one adds a quantum correction at the harmonic level to the Wigner–Kirkwood expression

$$Q_{tor}^{MPG} = \left(\frac{Q_{tor}^{HO}}{Q_{tor}^{WKHO}}\right)Q_{tor}^{WK}, \tag{41}$$

where Q^{WKHO} is the Wigner–Kirkwood approximation for a harmonic oscillator,

$$Q_{tor}^{WKHO} = \frac{1}{\hbar\beta\omega} + \frac{\hbar\beta\omega}{24}. \tag{42}$$

IV.D.3. Displaced-points path integrals

The displaced-points path integral (DPPI) methods[48] with either harmonic sampling (DPPI-HS) or anharmonic sampling (DPPI-AS) are also affordable choices, and may be viewed as approximate anharmonic corrections beyond the PG approximation [see Eq. (45) of Mielke and Truhlar[48]]. We note that DPPI-HS is particularly attractive when computational cost is a strong factor because, aside from convergence considerations, it is only about a factor of 2 more expensive than a classical phase-space integral. For a one-dimensional torsion, the DPPI-HS approximation for the partition function is calculated via

$$Q^{TDPPI-HS} = \frac{(2\pi kIT)^{1/2}}{2\pi\hbar} \int_0^{2\pi/\sigma} d\phi \exp\left(-\frac{\beta}{2}\{V[\phi + c/2] + V[\phi - c/2]\}\right), \tag{43}$$

where the initial T in the acronym denotes that the path integral is applied in one dimension to only the torsional degree of freedom,

$$C = \left[\frac{8}{\beta k} \ln \frac{\sinh(\beta\hbar\omega/2)}{\beta\hbar\omega/2}\right]^{1/2}, \tag{44}$$

and where k is defined in Eq. (13). The TDPPI-AS approximation for the partition function is calculated similarly to Eq. (43) except that k and hence the parameter c are ϕ dependent and c is evaluated via Eq. (44) with

$$k(\phi) = \frac{d^2V}{d\phi^2} \tag{45}$$

if k is positive, and otherwise via

$$c = \sqrt{\frac{8}{\beta k} \ln \kappa}, \qquad (46)$$

where k is given by

$$\kappa = \begin{cases} \dfrac{\pi\beta/\alpha}{\sin(\pi\beta/\alpha)} + \dfrac{\beta}{\beta-\alpha}\exp[(\beta-\alpha)V] & (\beta < \alpha) \\[2mm] \beta V & (\beta = \alpha) \\[2mm] \dfrac{\beta}{\beta-\alpha}\{-1 + \exp[(\beta-\alpha)V]\} & (\beta > \alpha) \end{cases}$$

$$(47)$$

and

$$\alpha = \frac{2\pi}{\hbar|d^2V/d\phi^2|}. \qquad (48)$$

If the accurate one-dimensional potential is unavailable, the TDPPI-HS method may be used with the segmented reference potential implicit in Eq. (34); this provides a more accurate estimate of quantum effects than the SRPG scheme; we will denote this method as SR-TDPPI-HS. The SR-TDPPI-HS method only requires geometries, frequencies, and barrier heights.

IV.E. Estimates for the effective reduced moment of inertia

Numerous approaches have been presented for the calculation of effective reduced moments of inertia $I_{\text{tor},j}$ at a given torsional minimum j.[4,5,9,10,49,50] The use of an effective value for I in the 1D torsion treatments, rather than accounting for the geometry dependence, constitutes an approximation in the way we choose to model the full-D torsional effects; the TES calculations will provide us with an exact treatment of this 1D model that we may use to benchmark further approximations. We will consider only five moment schemes in this paper, to be labeled C, R, ωk, CAF, and CAR. The first is the method of Pitzer,[5] based in part on the earlier work of Pitzer and Gwinn[4] but superseding it. The Pitzer method will be referred to as the C or curvilinear scheme. The second is a method of Truhlar,[9] which will be referred to as the R or rectilinear scheme, and the third, which we will denote the ωk or frequency scheme, selects I so that the harmonic frequency $\bar{\omega}$ for the 1D potential of Eq. (1) matches the harmonic torsional frequency ω of the full-dimensional system, i.e., we set

$$I^{\omega k} = \frac{2k}{\omega^2}, \qquad (49)$$

where the force constant k is defined in Eq. (13).

The C scheme[5] involves a complicated calculation to decouple overall rotation from the internal rotation, and we refer the reader to the EPAPS supplement for the full details. As is customary, we set the internal rotation axis used in the C scheme to the O–O bond axis; we note that other axis choices have been advocated elsewhere.[10] The R scheme[9] attempts to account for the axis selection issue by calculating the angular momentum vector of each subrotator from the normal mode eigenvector for the torsion and then defining
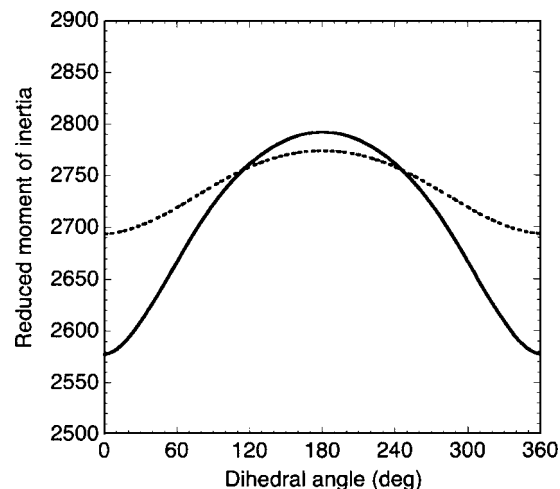

FIG. 2. The C scheme moment of inertia (in $m_e a_0^2$) for H_2O_2 calculated as a function of the torsional coordinate with all other coordinates frozen at their equilibrium values (dotted line) and with all other coordinates optimized (solid line).

the axis of rotation by shifting this vector to pass through the center of mass. This scheme yields a reasonable rotation axis for slightly off-balance internal rotations, such as the one in H_2O_2, but has been shown[18] to yield highly inaccurate values for molecules where the center of mass of either fragment is far from the bond axis—as will frequently occur for large molecules.

In the standard C scheme one evaluates I at the minimum-energy configuration. We also consider two curvilinear-averaged (CA) schemes in which I is obtained by integrating over ϕ,

$$I^{\text{CA}} = \left[\left(\frac{\sigma}{2\pi}\right)\int_0^{2\pi/\sigma}[I_{\text{tor}}^{\text{C}}(\phi)]^{1/2}d\phi\right]^2. \qquad (50)$$

The curvilinear reduced moment of inertia as a function of the torsion angle for H_2O_2 is plotted in Fig. 2. Two cases are considered; in the first the torsion angle was varied while the other bond lengths and angles remained fixed at their values for the minimum structure; this is called the CA-frozen (CAF) scheme. In the second the other coordinates were optimized, which is called the CA-relaxed (CAR) scheme. Figure 2 shows that the reduced moment of inertia varies by at most 8% as the torsion angle changes if the other coordinates are optimized and by at most 3% if these coordinates are not optimized.

Table II lists moments of inertia for various isotopomers as calculated via the C, CAF, CAR, ωk, and R schemes. The values of I obtained from the equilibrium configuration (C scheme) differ by at most 2.8% from the effective moments from Eq. (50). Therefore, if one accepts that the curvilinear method adequately accounts for the ϕ dependence, the use of a constant reduced moment of inertia in all calculations presented in this paper is a good approximation.

IV.F. 1D Zero-point energy corrections

The zero-point energy corrected partition function for the torsional mode for method X is defined as

TABLE II. Moments of inertia (in $m_e a_0^2$) calculated by five approximate schemes for various isotopomers of H_2O_2.

System	C	CAR	CAF	ωk	R
H_2O_2	2754.9	2704.8	2737.3	2764.9	3875.2
D_2O_2	5181.0	5037.5	5114.0	5165.7	7586.3
HOOD	3597.1	3519.6	3565.8	3599.7	5366.8
$D^{18}OOH$	3614.0	3538.6	3584.2	3617.0	5391.0
$H^{18}OOD$	3613.4	3538.2	3583.8	3617.0	5351.8
$H^{18}OOH$	2764.8	2716.1	2748.2	2775.1	3886.5
$H_2^{18}O_2$	2774.8	2727.4	2759.1	2786.8	3898.0

$$Q_{\text{tor}}^{X\text{-}Z} = \exp[\beta(E_{\text{tor},0}^X - E_{\text{tor},0})]Q_{\text{tor}}^X, \tag{51}$$

where $E_{\text{tor},0}$ is the numerically converged separable ground-state torsional energy, which we obtain from exact 1D torsional eigenvalue calculations, as discussed in Sec. IV.D, and $E_{\text{tor},0}^X$ is the approximate separable zero-point torsional energy predicted by method X.

V. NONSEPARABLE APPROXIMATIONS

A number of nonseparable approximations were considered in Ref. 31. In the present paper we will consider only two simple types of nonseparable approximations—namely, zero-point energy corrections and a hybrid form of the multidimensional Pitzer–Gwinn approximation where the QM correction includes the effects of torsion.

V.A. Full-dimensional zero-point energy corrections

The first set of nonseparable approximations we consider in the present paper is based on taking account of the accurate nonseparable ZPE. In particular, if Q^X denotes a partition function of a separable method that uses a ZPE of $E_{\text{tor},0}^X$ for the torsional mode and harmonic treatments for the other modes, we define the zero-point-corrected partition function of method X by

$$Q^{X\text{-}Z} = \exp[\beta(E_0^X - E_0)]Q^X, \tag{52}$$

where

$$E_0^X = E_{\text{tor},0}^X + \sum_{m \neq 4} \hbar\omega_m/2 \tag{53}$$

and E_0 is the accurate ZPE, as already mentioned in Sec. II. Except for the TES and MFG schemes, all methods where we consider ZPE corrections have an $E_{\text{tor},0}^X$ that is simply the harmonic ZPE. The TES scheme uses the lowest eigenvalue of the 1D potential of Eq. (1) for $E_{\text{tor},0}^{\text{TES}}$. Accurate values of E_0 are available from the calculations of Koput *et al.*[51,52] for H_2O_2 (5726.1 cm^{-1}), D_2O_2 (4326.2 cm^{-1}), HOOD (5028.8 cm^{-1}), and $H_2^{18}O_2$ (5681.7 cm^{-1}). Based on these values, reasonable estimates of accurate ZPEs were also obtained[31] for $H^{18}OOH$ (5704.1 cm^{-1}), $D^{18}OOH$ (5003.5 cm^{-1}), and $H^{18}OOD$ (5006.0 cm^{-1}) that are expected to be accurate to within 1–2 cm^{-1}.

V.B. Improved-reference Pitzer–Gwinn approximation for molecules with torsions

We can use the results of the 1D eigenvalue summation to create an improved-reference Pitzer–Gwinn (IRPG) method where the quantum correction of the (coupled full-dimensional) classical phase-space integral is obtained at the HO+T level rather than the HO level. In this method a harmonic reference is used for nontorsional modes, as in the original PG method, but is replaced by an accurate one-dimensional reference for the torsion. In particular, we use the hindered-rotator vibrational partition functions with mode 4 treated by eigenvalue summation for the QM case and treated by Eq. (14) for the classical case. This yields

$$Q^{\text{IRPG}} = Q^{\text{classical}}\frac{Q_{\text{vib}}^{\text{HO+TES}}}{Q_{\text{vib}}^{\text{CHO+T}}}, \tag{54}$$

where $Q^{\text{classical}}$ is the classical approximation to the nonseparable vibration-rotation partition function,

$$Q_{\text{vib}}^{\text{HO+TES}} = Q_{\text{tor}}^{\text{TES}}Q_{\text{sb}}^{\text{HO}}, \tag{55}$$

and

$$Q_{\text{vib}}^{\text{CHO+T}} = Q_{\text{tor}}^{\text{classical}}\prod_{m=1-3,5,6}\frac{1}{\hbar\beta\omega_m}. \tag{56}$$

VI. RESULTS AND DISCUSSION

VI.A. One-dimensional tests for H_2O_2

The first issue we need to address is the best way to estimate the reduced moment of inertia. For H_2O_2, the ωk, C, and R schemes predict I values of 2764.9, 2754.9, and 3875.2$m_e a_0^2$, respectively. The 0.4% difference between the ωk scheme and C scheme values is less than the variation of I with geometry, but the R scheme value differs from the results of the other two methods by ~40%. In Table III we compare frequencies, relative to the ground state, obtained by diagonalizing the 1D Hamiltonian with these moments of inertia to the frequencies Koput *et al.*[52] report for the full-dimensional system. The eigenvalues obtained with the ωk and C schemes agree with those of the full-dimensional results to within mean unsigned differences of 7.0 and 9.4 cm^{-1}, respectively; but the R scheme performs poorly, with a mean unsigned difference with the full-dimensional results of 210 cm^{-1}. Therefore, for the remainder of the calculations presented here (that is, in the printed portion of this

TABLE III. Comparison of eigenvalues of the 1D effective torsional potential obtained with three different estimates of the reduced moment of inertia for H_2O_2 (in cm^{-1} and relative to the ground state) with the results of Koput et al. with the full-dimensional potential.

ωk scheme	C scheme	R scheme	Full-D[a]
12.7	12.8	5.1	9.9
252.8	253.2	225.5	261.2
373.5	374.4	299.6	371.6
573.6	575.1	461.1	571.1
782.1	784.1	621.6	776.2
1008.2	1010.7	801.7	1000.8
1243.6	1246.6	991.5	1229.2
1483.6	1487.1	1188.8	1479.3
1727.2	1731.2	1391.0	1721.0
1954.8	1958.8	1594.9	1948.6
2210.4	2215.3	1799.9	2208.0
2343.9	2347.5	1993.8	2322.4

[a]Koput et al., Ref. 32.

TABLE IV. Harmonic frequencies, zero-point energies (ZPE), anharmonic ZPE corrections, and tunneling splittings (all in cm^{-1}) for various isotopomers of H_2O_2.

Molecule	ω (full-D)[a]	ω (1D)[b]	ZPE$_{tor}$[c]	ΔZPE[d]	Splitting[e]
H_2O_2	381.9	382.6	168.3	−23.0	12.8
D_2O_2	279.4	279.0	130.1	−9.4	2.0
HOOD	334.7	334.8	151.8	−15.6	6.3
$H_2^{18}O_2$	380.4	381.2	167.9	−22.7	12.6
D^{18}OOH	333.9	334.0	151.5	−15.5	6.2
H^{18}OOH	381.2	381.9	168.1	−22.8	12.7
H^{18}OOD	333.9	334.1	151.6	−15.5	6.3

[a]Harmonic frequency for the torsion mode from normal mode analysis with the full-D potential.
[b]Harmonic frequency for the 1D potential with a C scheme moment of inertia.
[c]From accurate 1D diagonalization of the potential of Eq. (1) with reduced moment of inertia determined by the C scheme at the equilibrium geometry.
[d]$(1/2)\hbar\,\omega(1D) - \text{ZPE}_{tor}$.
[e]Tunneling splitting for the 1D effective potential from accurate 1D diagonalization of the potential of Eq. (1) with reduced moment of inertia determined by the C scheme at the equilibrium geometry.

article) we will only consider the C scheme moment of inertia, but we will present results for the R scheme in the supplementary material.[53]

Table IV presents, for the seven isotopomers considered here, harmonic frequencies, zero-point energies, anharmonic zero-point energy corrections, and tunneling splittings, with the last three columns determined by diagonalizing the 1D system with I values taken from the C scheme at the minimum configuration. Where applicable, we will consider approximate partition function estimates both with and without a correction for the ZPE anharmonicity. When correcting for ZPE effects in this section, we will use the accurate one-dimensional ZPE corrections, and will distinguish these data by adding a −Z to the method name. We note that the ZPE correction scheme of McClurg et al.[12] was not derived to treat general potentials, and the authors specifically mentioned H_2O_2 as a potential that may not be appropriate for their method, so we will not consider their approximate ZPE correction scheme (or any other approximate ZPE scheme) in the remainder of this paper. Tunneling splitting will have a significant effect at very low temperatures (such as the lowest T value of 200 K studied here), but many of the approximate methods do not correctly account for this effect. At all but the highest T value the contributions to the partition function from above the upper torsional barrier is reasonably small. At 1000, 1500, 2400, and 5000 K for H_2O_2, contributions from eigenvalues above the barrier in the exact 1D results are 1%, 5%, 13%, and 31%, respectively.

Table V compares partition functions for the 1D torsional potential of H_2O_2 obtained by eigenvalue summation with those of 15 approximate methods and 7 methods augmented with one-dimensional ZPE corrections. Table VI considers H_2O_2/D_2O_2 isotope ratios obtained for the 1D torsional potential. Table VII lists mean unsigned percentage errors (MU%E), averaged over the nine T values for the seven isotopologs, for the various methods sorted in order of increasing MU%E.

Table VII shows that none of the three interpolatory methods, or their ZPE corrected analogs, proposed by Chuang and Truhlar, perform well. The CW scheme is especially inaccurate at low T and has the largest MU%E of any of the methods considered here, and the ωW scheme is especially inaccurate at high T. When the geometries, frequencies, and barrier heights are known, there are better options than the Chuang and Truhlar interpolations. However, in cases where only the geometries and frequencies are known, the Cω interpolatory scheme of CT is indeed a better option than MC-HO. As expected, the MC-HO and MC-HO-Z methods do poorly, but since even at the highest temperatures the partition functions are dominated by contributions from below the higher torsion barrier, these methods are not vastly inferior to some of the methods that treat hindered-rotation approximately.

Four of the geometry, frequency, and barrier height schemes considered here use segmented reference potentials to approximate the full potential based only on information at relative maxima and minima. These include the SRC, SRPG, SAS, and SR-TDPPI-HS methods. These methods involve an amount of work that is comparable to that of the various CT, RPG, and MC-HO schemes, but they use a more realistic potential. The approximation of the true potential involves a certain intrinsic error; a crude measure of this can be seen by comparing the SRC results with the accurately integrated classical results and the SR-TDPPI-HS results to the TDPPI-HS results. The SRC partition functions for H_2O_2 are systematically 2%–4% lower than $Q^{classical}$, and these deviations hold almost exactly for the TDPPI schemes except at the lowest temperature. The SAS scheme performs comparably to the SRPG scheme at low T, but at moderate to higher temperatures it is systematically marginally better for all but the highest T value (5000 K). Unfortunately, the SAS scheme cannot easily be corrected for ZPE errors because the correction factor already partially corrects for this deficiency. The SR-TDPPI-HS method is slightly more expensive than the other four methods of this class because it requires a numerical integration of the reference potential. Because the reference potential is fairly inexpensive to evaluate, this ad-

TABLE V. Partition functions for the 1D torsional potential of H_2O_2 calculated using various methods.

T (K)	200	300	400	600	1000	1500	2400	5000
Methods that require geometries and frequencies								
CT-Cω	0.541	0.952	1.343	2.087	3.474	5.051	7.540	13.115
MC-HO	0.541	0.953	1.347	2.109	3.595	5.429	8.717	18.190
Method that require geometries, frequencies, and barrier heights								
SAS	0.566	1.023	1.464	2.308	3.818	5.428	7.846	13.188
SRC	0.762	1.167	1.560	2.302	3.662	5.216	7.701	13.301
SR-TDPPI-HS	0.601	1.056	1.479	2.252	3.637	5.203	7.695	13.300
SRPG	0.566	1.018	1.444	2.223	3.616	5.187	7.684	13.295
CT-ωW	0.541	0.953	1.347	2.104	3.553	5.268	8.107	14.871
CT-CW	0.364	0.698	1.019	1.631	2.791	4.156	6.408	11.767
RPG	0.440	0.788	1.137	1.852	3.312	5.041	7.744	13.558
Methods that require the whole 1D potential								
TDPPI-HS	0.642	1.114	1.554	2.358	3.786	5.381	7.891	13.488
WK	0.626	1.110	1.553	2.358	3.786	5.382	7.892	13.488
MPG	0.679	1.126	1.560	2.360	3.787	5.382	7.892	13.488
TDPPI-AS	0.609	1.105	1.550	2.357	3.786	5.381	7.891	13.488
TPG	0.591	1.065	1.510	2.324	3.763	5.365	7.880	13.483
Classical	0.796	1.220	1.632	2.406	3.811	5.395	7.897	13.489
Methods that require geometries and frequencies and the ZPE								
CT-Cω-Z	0.636	1.061	1.457	2.204	3.588	5.162	7.643	13.200
MC-HO-Z	0.637	1.062	1.462	2.227	3.713	5.548	8.836	18.309
Methods that require geometries, frequencies, barrier heights, and the ZPE								
SRPG-Z	0.666	1.135	1.566	2.347	3.736	5.301	7.789	13.382
CT-$W\omega$-Z	0.637	1.062	1.461	2.221	3.670	5.384	8.218	14.968
CT-CW-Z	0.428	0.778	1.105	1.722	2.883	4.247	6.496	11.843
RPG-Z	0.518	0.878	1.233	1.955	3.421	5.151	7.850	13.647
Methods that require the whole 1D potential and the ZPE								
TPG-Z	0.696	1.187	1.638	2.453	3.888	5.482	7.987	13.571
Accurate eigenvalue summation								
TES	0.644	1.116	1.555	2.358	3.786	5.382	7.892	13.488

ditional cost will typically not be a deciding factor, in which case the SR-TDPPI-HS approach should be the most reliable of this class of methods.

Seven of the schemes considered here require accurate numerical integration of a 1D integral involving the accurate torsion potential—the classical, torsional PG, torsional PG-Z, WK, MPG, TDPPI-HS, and TDPPI-AS methods. The classical phase-space integral result does very well for $T \geqslant 600$ K, and for H_2O_2 (the most challenging case) it is only in error by 24%, 9%, and 5% at $T=200$, 300, and 400 K, respectively. The Wigner–Kirkwood method does extremely well at all but the lowest temperature, and even at 200 K the error is only 3%. The MPG scheme seems to produce results that are systematically inferior to the WK results that it is intended to correct, so it is not recommended. The TDPPI-AS scheme does nearly as well as the WK approach, and the TDPPI-HS scheme is easily the best performing method, with the worst error being only 0.3% at 200 K. The TPG scheme performs relatively well, although it systematically underestimates the partition function while the TPG-Z scheme systematically overestimates the partition function and is slightly less accurate on balance than the TPG results. This is partly a consequence of the harmonic partition func-

tion only characterizing the lowest few (two for H_2O_2) eigenvalues well—since these are the only ones that are below the lower barrier. If the barrier heights were less uneven the TPG-Z scheme would be expected to perform better.

If potential evaluations are expensive compared with some of the other work that needs to be done, these seven methods might not be affordable. Nevertheless it is interesting to learn from Table VII, that of these seven methods requiring accurate numerical quadratures of the torsional potential, the TDPPI-HS scheme is a clear favorite as it is the most accurate while being less expensive than all but the classical method (and only about a factor of 2 more expensive than that method). For some model 1D problems, and especially in multidimensional problems, the TDPPI-AS scheme has been observed to perform better than the TDPPI-HS scheme.[48] For the cases tested so far, this tends to occur at low temperatures when the classical approximation is significantly less accurate than it is here. It is possible that the TDPPI-HS scheme will tend to outperform the TDPPI-AS scheme in the nearly classical regime for 1D problems, but it is also possible that the extremely high accuracy of the TDPPI-HS scheme observed here is partially fortuitous.

TABLE VI. H_2O_2/D_2O_2 isotope ratios for partition functions of the 1D torsional potential using various methods.

T (K)	200	300	400	600	1000	1500	2400	5000
Methods that require geometries and frequencies								
CT-Cω	0.640	0.687	0.706	0.720	0.727	0.729	0.730	0.730
MC-HO	0.640	0.688	0.706	0.720	0.727	0.730	0.731	0.731
Methods that require geometries, frequencies, and barrier heights								
SAS	0.638	0.687	0.707	0.725	0.735	0.737	0.736	0.733
SRC	0.729	0.729	0.729	0.729	0.729	0.729	0.729	0.729
SR-TDPPI-HS	0.658	0.697	0.712	0.722	0.727	0.728	0.729	0.729
SRPG	0.638	0.685	0.704	0.717	0.725	0.727	0.728	0.729
CT-ωW	0.640	0.688	0.706	0.720	0.727	0.730	0.731	0.731
CT-CW	0.594	0.662	0.689	0.710	0.722	0.726	0.728	0.729
RPG	0.638	0.685	0.704	0.718	0.725	0.727	0.728	0.729
Methods that require the whole 1D potential								
TDPPI-HS	0.664	0.700	0.713	0.722	0.727	0.728	0.729	0.729
WK	0.653	0.698	0.713	0.722	0.727	0.728	0.729	0.729
MPG	0.694	0.705	0.715	0.723	0.727	0.728	0.729	0.729
TDPPI-AS	0.639	0.696	0.712	0.722	0.727	0.728	0.729	0.729
TPG	0.638	0.685	0.704	0.718	0.725	0.727	0.728	0.729
Classical	0.730	0.729	0.729	0.729	0.729	0.729	0.729	0.729
Methods that require geometries and frequencies and the ZPE								
CT-$C\omega$-Z	0.703	0.731	0.740	0.743	0.741	0.739	0.737	0.734
MC-HO-Z	0.703	0.732	0.740	0.743	0.741	0.738	0.736	0.733
Methods that require geometries, frequencies, barrier heights, and the ZPE								
SRPG-Z	0.700	0.729	0.737	0.740	0.739	0.736	0.734	0.732
CT-$W\omega$-Z	0.703	0.732	0.740	0.743	0.741	0.739	0.737	0.734
CT-CW-Z	0.651	0.704	0.722	0.733	0.736	0.735	0.734	0.732
RPG-Z	0.701	0.729	0.737	0.740	0.739	0.736	0.734	0.732
Methods that require the whole 1D potential and the accurate ZPE								
TPG-Z	0.701	0.730	0.738	0.740	0.739	0.736	0.734	0.732
Accurate eigenvalue summation								
TES	0.665	0.701	0.713	0.722	0.727	0.728	0.729	0.729

VI.B. One-dimensional tests for isotope effects

Next we turn to the evaluation of isotope effects (of the 1D potential); the H_2O_2/D_2O_2 isotope ratios are the most difficult to obtain accurate values for so we will concentrate on those data. A number of trends may be discerned *a priori*. Since isotope effects are a quantal phenomenon the classical and SRC results do not predict these quantities accurately (results for these two methods are identical and T independent). As discussed previously[31] it is easy to show (using the Teller-Redlich product rule) that the Pitzer–Gwinn and HO isotope ratios are identical, and it is also straightforward to show that the MC-HO, TPG, SRPG, $I\omega$, and ωW methods will yield results identical to the HO ones provided that the moments of inertia are calculated in the ωk scheme and only a single frequency is present in the MC-HO expression (in the ωk scheme, Q_{FR} has an identical mass dependence to that of Q_{HO}). The strong similarity of the C scheme moments of inertia to those computed by the ωk scheme ensures that the isotope ratio calculations for all methods in this class will also be of similar quality. Since all of these methods only include quantum effects at the harmonic level their accuracy for isotope-effect predictions can be expected to be of similar

quality under more general conditions. Similarly, the isotope ratios of the MC-HO-Z, $I\omega$-Z, ωW-Z, SRPG-Z, and TPG-Z methods all predict identical isotope ratios for this molecular system when the moments of inertia are calculated in the ωk scheme and are very similar when the C scheme is used.

The ZPE correction actually degrades the quality of the isotope-effect predictions, with the ZPE corrected methods overestimating the accurate values by more than the uncorrected methods underestimate the accurate values (except for the CW method, which displays irregular and extremely poor behavior). The SAS, CW, and CW-Z methods all perform less accurately than the MC-HO schemes and have less regular trends than the other methods.

Five approaches do better than the crude MC-HO isotope ratios—TDPPI-HS, SR-TDPPI-HS, WK, TDPPI-AS, and MPG. As in the case of the partition function values, MPG is systematically slightly inferior to WK, and TDPPI-AS is systematically slightly inferior to TDPPI-HS. The one interesting finding is that the SR-TDPPI-HS method does extremely well for isotope effects even though it does not fare nearly as well for the individual partition functions

TABLE VII. Percentage errors for 1D. [Mean unsigned percentage errors (MU%E) and maximum percentage errors (Max%E) averaged over nine temperatures in the rage of 200-5000 K for all seven isotopomers for 1D torsional partition functions with moments of inertia obtained from the C scheme at the minimum configuration. The results, for a given amount of data, are sorted in order of increasing MU%E.]

Method of type of method	Abbreviation	MU%E	Max%E
Methods that require geometries and frequencies			
Interpolatory	CT-Cω	9.4	16.0
Harmonic	MC-HO	12.3	34.9
Methods that require geometries, frequencies, and barrier heights			
Segmented AS	SAS	3.4	12.1
Segmented classical	SRC	3.8	18.3
Path integral	SR-TDPPI-HS	4.0	6.7
Segmented Pitzer–Gwinn	SRPG	5.3	12.1
Interpolatory	CT-$W\omega$	9.1	16.0
Reference PG	RPG	16.1	31.7
Interpolatory	CT-CW	27.7	43.5
Methods that require the whole 1D potential			
Path integral	TDPPI-HS	0.05	0.4
Wigner-Kirkwood	WK	0.3	2.8
Modified Pitzer–Gwinn	MPG	0.5	5.4
Path integral	TDPPI-AS	0.5	5.5
Torsinal Pitzer–Gwinn	TPG	1.8	8.2
Classical	Classical	3.9	23.5
Methods that require geometries and frequencies and the ZPE			
Corrected interpolatory	CT-Cω-Z	5.3	9.6
Corrected harmonic	MC-HO-Z	8.9	35.8
Methods that require geometries, frequencies, barrier heights, and the ZPE			
Corrected segmented PG	SRPG-Z	1.5	3.4
Corrected interpolatory	CT-$W\omega$-Z	5.3	11.0
Corrected reference PG	RPG-Z	12.6	24.4
Corrected interpolatory	CT-CW-Z	24.7	33.5
Methods that require the whole 1D potential and the ZPE			
Corrected Pitzer–Gwinn	TPG-Z	2.8	8.0

TABLE VIII. Mean unsigned percentage errors (MU%E) (averaged over seven temperatures in the range of 300–2400 K for all seven isotopomers) and maximum percentage errors (Max%E) full-dimensional molecular partition functions for the torsional mode treated by various methods with moments of inertia obtained from the C scheme at the minimum configuration, and the other modes treated at the quantum HO level. The results, for a given amount of data, are sorted in order of increasing sum of MU%E and Max%E.

Method or type of method	Abbreviation	MU%E	Max%E
Methods that require geometries and frequencies			
Harmonic	MC-HO	28	46
Interpolatory	CT-Cω	31	46
Methods that require geometries, frequencies, and barrier heights			
Segmented classical	SRC	25	34
Segmented AS	SAS	25	42
Path integral	SR-TDPPI-HS	27	40
Segmented Pitzer–Gwinn	SRPG	27	42
Interpolatory	CT-$W\omega$	29	46
Reference Pitzer–Gwinn	RPG	36	55
Interpolatory	CT-CW	45	61
Methods that require the whole 1D potential			
Classical	Classical	22	31
Modified Pitzer–Gwinn	MPG	23	36
Eigensummation	TES	24	37
Path integral	TDPPI-HS	24	37
Wigner–Kirkwood	WK	24	37
Path integral	TDPPI-AS	24	37
Pitzer–Gwinn	TPG	24	40
Methods that require geometries and frequencies and the ZPE			
Corrected harmonic	MC-HO-Z	12	16
Interpolatory	CT-Cω-Z	15	27
Methods that require geometries, frequencies, barrier heights, and the ZPE			
Corrected interpolatory	CT-$W\omega$-Z	13	22
Corrected segmented PG	SRPG-Z	11	25
Corrected segmented PG	RPG-Z	22	26
Corrected interpolatory	CT-CW-Z	33	38
Methods that require the whole 1D potential and the ZPE			
Corrected Pitzer–Gwinn	TPG-Z	8	24
Corrected eigensummation	TES-Z	9	24

due to intrinsic errors in approximating the torsional potential by a simple segmented reference potential.

The reader should keep in mind that although the 1D tests are very informative at a fundamental level, the 1D problem is itself an imperfect representation of the actual torsion as it occurs in the full coupled-mode molecule, and the assumption of a constant torsional moment of inertia makes the 1D schemes considered here even more artificial.

VI.C. Full molecular partition functions calculated by HO+T methods

Next we consider the accuracy of approximate methods when compared with the full-dimensional partition functions. These are the key results of the present paper, and so we start with a table like Table VII but now for the full partition coefficient; these results are in Table VIII. All results in Table VIII are averaged over all seven isotopologs at seven temperatures, for a total of 49 cases. (The temperatures are 300, 400, 600, 800, 1000, 1500, and 2400 K.) We note that the accurate path integral results include both intermode cou-

pling of vibrations and vibration-rotation coupling; they are available for seven of the nine temperatures considered in the 1D calculations (200 and 5000 K, the highest and lowest of the T values previously considered, are dropped in Table VII). We also note that even when classical approximation methods are used to treat the torsional mode, all other degrees of freedom are treated using the quantal harmonic approximation.

The most striking observation that may be made concerning the statistical errors in Table VIII is that they are considerably larger than those observed for the 1D calculations. Partly, this is due to the much larger effects of anharmonicity on the ZPE, but even when the TES approach is corrected to reflect the accurate multidimensional ZPE, the MU%E only drops from 23.5% to 9.3%. The tabulated methods either neglect mode-mode coupling completely or (in the case of the ZPE corrected schemes) have only a limited treat-

TABLE IX. Mean unsigned percentage errors (MU%E) (averaged over seven temperatures in the range 300–2400 K for all seven isotopmers) and maximum percentage errors (Max%E) for full-dimensional molecular partition functions for methods that require the whole multidimensional surface.

Method or type of method	Abbreviation	MU%E	Max%E
Methods that require the multidimensional potential			
Improved-reference PG	IRPG	14	35
Corrected IRPG	IRPG-Z	1	2

TABLE X. Comparison of mean unsigned percentage errors in 1D and full-D for best methods in each class (for this purpose, "best" is defined as smallest MU%E or smallest Max%E).

Method or type of method	Abbreviation	Full-D	1D
Methods that require geometries and frequencies			
Harmonic	MC-HO	28	12
Interpolatory	CT-Cω	31	9
Methods that require geometries, frequencies, and barrier heights			
Segmented AS	SAS	25	3
Segmented classical	SRC	25	4
Path integral	SR-TDPPI-HS	27	4
Methods that require the whole 1D potential			
Classical	Classical	22	4
Path integral	TDPPI-HS	24	0.05
Methods that require the multidimensional potential			
Improved-reference PG	IRPG	14	⋯
Methods that require geometries, frequencies, and the ZPE			
Interpolatory	CT-Cω-Z	15	5
Corrected harmonic	MC-HO-Z	12	9
Methods that require geometries, frequencies, barrier heights, and the ZPE			
Corrected segmented PG	SRPG-Z	11	2
Interpolatory	CT-$W\omega$-Z	13	5
Methods that require the whole 1D potential and the ZPE			
Corrected Pitzer–Gwinn	TPG-Z	8	3
Methods that require the multidimensional potential and the ZPE			
Corrected IRPG	IRPG-Z	1	⋯

ment of this coupling, and they also contain significant errors associated with the anharmonic effects in the other five coordinates—which are only treated at the HO level. At the highest temperatures all of the separable and ZPE corrected separable methods significantly underestimate the accurate partition function. Several torsional treatments that overestimate the results of the 1D torsional potential profit from a fortuitous cancellation of errors whereby errors in the torsional treatment cancel errors from anharmonicity effects in the other five modes.

Table VIII shows that for the full-D calculations the advantage of using higher-level methods is modest in that the schemes that require geometries and frequencies are almost as good as the schemes that also require barrier heights, and the schemes that require the accurate 1D potential are only slightly better. The only way to drop the maximum percentage error below 31% is to use the accurate ZPE.

VI.D. Full molecular partition functions calculated by IRPG methods

Table IX shows the results for the IRPG and IRPG-Z methods, which include mode-mode coupling via a full-dimensional phase-space integral. Unless the accurate ZPE is utilized, the IRPG method is only moderately better than the HO+T methods. The IRPG-Z method, which accounts for mode-mode coupling and uses the accurate ZPE, has a MU%E and Max%E of 1% and 2%, respectively, which makes it the only method tested that has a Max%E of less than 15%.

VI.E. Overall comparison of the best methods

Table X compares the errors for the 1D problem with the errors for the full-D problem. (Table X shows only a subset of the methods, namely, those that, for a given amount of data required, have the smallest error in either MU%E or Max%E for either the 1D or the full-D problem.) The top half of Table X (methods not using the accurate ZPE) shows that the errors for the full vibrational partition function are much larger than the errors for the separable torsion. Thus, if the goal of the calculation is obtaining the most accurate absolute partition function, an improved separable treatment of the torsion that retains harmonic approximations for the other modes does not offer dramatic improvement (at least for H_2O_2, where the mean unsigned percentage error in the 1D MC-HO partition functions is only 12%). However, in applications such as rate constant calculations one often finds that the characteristics of most of the high-frequency mo-

tions do not vary significantly between the reactant and transition state; thus, anharmonicity errors in the rate constant from these modes may largely cancel, in which case errors from the torsional treatment may still be the leading source of concern. Even in such a case though, it is still not clear whether a separable treatment of the torsion can make the overall rate constant more accurate, especially when the torsion appears in the transition state but not in the reactant, because one is still neglecting coupling of the torsion to other vibrational modes and to rotation. (We also note that the typical harmonic approximation, which does not account for the multiple conformers, would be in error by an additional factor of 2, resulting in an error in the partition function varying from a factor of 2.3 at 300 K to 2.2 at 800 K and 1.8 at 2400 K.) When an accurate nonseparable zero-point energy is used, the more accurate methods yield good results at low T, but only the IRPG scheme performs well at high temperatures where anharmonicity in the nontorsional modes and mode-mode coupling become important considerations.

VII. CONCLUDING REMARKS

Most approximate methods for treating torsions have been designed for cases, such as the rotation of methyl groups, where the heights and spacings of the torsion barriers

are equal; neither of these two assumptions holds for the torsional motion in H_2O_2 so the system is an excellent case to use in testing methods intended for general problems. H_2O_2 is also the only system with a torsion of any kind for which accurate, full-dimensional quantal partition functions have been published for use as benchmarks.

We have examined 22 methods for calculating partition functions of one-dimensional torsional potentials. If the potential can be easily represented in a low-order Fourier series, the Hamiltonian takes the form of a banded matrix with analytically determinable matrix elements; for many applications such systems can often be affordably diagonalized and partition functions obtained via direct eigenvalue summation. When this approach is not feasible, but one can still afford to perform a numerical quadrature over the torsion coordinate, the TDPPI-HS method is the method of choice. If the potential is only known at the locations of the barriers and minima, then the segmented reference Pitzer–Gwinn scheme or the SR-TDPPI-HS method (which requires accurate integration involving only the segmented reference potential) are the most appropriate methods from among those considered here. For systems where only the geometries and frequencies are known, the CT-Cω method is best option. We also point out that the usual manner of applying the harmonic approximation would be in error by approximately a factor of 2, but once one recognizes the issue, this error is easily corrected without requiring additional data.

Zero-point energy (ZPE) anharmonicity has a large effect on the accuracy of approximate partition function estimates. If the accurate ZPE is taken into account, separable-approximation partition functions using the most accurate torsion treatment and harmonic treatments for the remaining degrees of freedom agree with accurate QM partition functions to within a mean accuracy of 9%. If no ZPE anharmonicity correction is used, the mean accuracy of the separable treatment drops to 23%.

We also presented a simple modification of the multidimensional Pitzer–Gwinn approximation, denoted the improved-reference Pitzer–Gwinn (IRPG) approximation, that includes an accurate treatment of a 1D torsional model instead of a harmonic treatment in the quantum correction to the full-dimensional classical phase-space integral. When an accurate ZPE correction is also employed, the IRPG method provides substantial improvements compared with the standard Pitzer–Gwinn approximation with the worst errors for H_2O_2 being only 1%.

ACKNOWLEDGMENTS

[1] K. S. Pitzer, *Quantum Chemistry* (Prentice-Hall, Englewood Cliffs, NJ, 1953).
[2] H. H. Nielson, Phys. Rev. **60**, 794 (1941).
[3] H. H. Nielson, *Handbook of Physics* (Springer, Berlin, 1959), Vol. 37/1, p. 173.
[4] K. S. Pitzer and W. D. Gwinn, J. Chem. Phys. **10**, 428 (1942).
[5] K. S. Pitzer, J. Chem. Phys. **14**, 239 (1946).
[6] W. H. Stockmayer, J. Chem. Phys. **27**, 321 (1957).
[7] P. Hui-yun, J. Chem. Phys. **87**, 4846 (1987).
[8] A. Chung-Phillips, J. Chem. Phys. **88**, 1764 (1988).
[9] D. G. Truhlar, J. Comput. Chem. **12**, 266 (1991).
[10] A. L. L. East and L. Radom, J. Chem. Phys. **106**, 6655 (1997).
[11] J. Gang, M. J. Pilling, and S. H. Robertson, Chem. Phys. **231**, 183 (1997).
[12] R. B. McClurg, R. C. Flagan, and W. A. Goddard III, J. Chem. Phys. **106**, 6675 (1997); **111**, 7165(E) (1999).
[13] W. Witschel and C. Hartwigsen, Chem. Phys. Lett. **273**, 304 (1997).
[14] P. Y. Ayala and H. B. Schlegel, J. Chem. Phys. **108**, 2314 (1998).
[15] V. D. Knyazev, J. Phys. Chem. A **102**, 3916 (1998).
[16] V. D. Knyazev and W. Tsang, J. Phys. Chem. A **102**, 9167 (1998).
[17] V. D. Knyazev, J. Chem. Phys. **111**, 7161 (1999).
[18] Y.-Y. Chuang and D. G. Truhlar, J. Chem. Phys. **112**, 1221 (2000); **121**, 7036(E) (2004); **124**, 179903(E) (2006).
[19] F. M. Fernandez, J. Phys. B **35**, 4933 (2002).
[20] R. Janoshek and M. J. Rossi, Int. J. Chem. Kinet. **34**, 550 (2002).
[21] V. Van Speybroeck, D. V. Neck, and M. Waroquier, J. Phys. Chem. A **106**, 9845 (2002).
[22] L. Catoire, M. T. Swihart, S. Gail, and P. Dagaut, Int. J. Chem. Kinet. **35**, 453 (2003).
[23] G. Katzer and A. F. Sax, Chem. Phys. Lett. **368**, 473 (2003).
[24] L. Masgrav, A. Gonzalez-Lafont, and J. M. Lluch, J. Comput. Chem. **24**, 701 (2003).
[25] L. Vereecken and J. Peeters, J. Chem. Phys. **119**, 5159 (2003).
[26] J. R. Barker and C. N. Shovlin, Chem. Phys. Lett. **383**, 203 (2004).
[27] G. Katzer and A. F. Sax, J. Comput. Chem. **26**, 1438 (2005).
[28] V. Van Speybroeck, P. Vansteenkiste, D. V. Neck, and M. Waroquier, Chem. Phys. Lett. **402**, 479 (2005).
[29] P. Vansteenkiste, D. V. Neck, V. V. Speybroeck, and M. Waroquier, J. Chem. Phys. **124**, 044314 (2006).
[30] V. A. Lynch, S. L. Mielke, and D. G. Truhlar, J. Chem. Phys. **121**, 5148 (2004).
[31] V. A. Lynch, S. L. Mielke, and D. G. Truhlar, J. Phys. Chem. A **109**, 10092 (2005); **110**, 5965(E) (2006);
[32] J. Koput, S. Carter, and N. C. Handy, J. Phys. Chem. A **102**, 6325 (1998).
[33] D. A. McQuarrie, *Statistical Mechanics* (Harper & Row, New York, 1973).
[34] J. Cioslowski, Chem. Phys. Lett. **136**, 515 (1987).
[35] M. Suhm and R. O. Watts, Phys. Rep. **204**, 293 (1991).
[36] R. N. Barnett and K. B. Whaley, J. Chem. Phys. **99**, 9730 (1993).
[37] A. D. Isaacson and D. G. Truhlar, J. Chem. Phys. **75**, 4090 (1981).
[38] R. B. McClurg (private communication).
[39] H. B. Schlegel (private communication).
[40] E. Hirota, J. Chem. Phys. **28**, 839 (1958).
[41] E. Hirota, J. Chem. Phys. **37**, 283 (1962).
[42] R. M. Lees, J. Chem. Phys. **59**, 2690 (1973).
[43] D. Smith, J. Chem. Phys. **72**, 1408 (1980).
[44] G. A. Guirgis, B. A. Barton, Jr., and J. R. Durig, J. Chem. Phys. **79**, 5918 (1983).
[45] J. A. Kunc, Mol. Phys. **101**, 413 (2003).
[46] E. P. Wigner, Phys. Rev. **40**, 749 (1932).
[47] J. G. Kirkwood, Phys. Rev. **44**, 31 (1933).
[48] S. L. Mielke and D. G. Truhlar, J. Chem. Phys. **115**, 652 (2001).
[49] J. E. Kilpatrick and K. S. Pitzer, J. Chem. Phys. **17**, 1064 (1949).
[50] D. R. Herschbach, H. S. Johnston, K. S. Pitzer, and R. E. Powell, J. Chem. Phys. **25**, 736 (1956).
[51] J. Koput (private communication).

[52] J. Koput, S. Carter, and N. C. Handy, J. Chem. Phys. **115**, 8345 (2001).

[53] See EPAPS Document No. E-JCPSA6-125-004628 for 63 pages of supplementary information including partition functions and isotope ratios for all isotopomers studied using both the C and R scheme moments of inertia, a specification of the C scheme, and a discussion of the MFG ZPE correction method. This document can be reached via a direct link in the online article's HTML reference section or via the EPAPS homepage (http://www.aip.org/pubservs/epaps.html).